Self-Actuating 3D Printed Packaging for Deployable Antennas

Ryan Bahr, Abdullah Nauroze, Wenjing Su, M. M. Tentzeris
Electrical and Computer Engineering
Georgia Institute of Technology
Atlanta, USA
rbahr3@gatech.edu, nauroze@gatech.edu, wsu36@gatech.edu, etentze@ece.gatech.edu

***Abstract*— In this paper we demonstrate the ability to use low-cost 3D printers to manufacture an ambulatory antenna at Ka bands with shape memory polymers to be used in an origami array. A focus on the manufacturing process and limitations is discussed. The antenna is metalized on the 3D printed dielectric substrate (polylactic acid) using direct print additive manufacturing to deposit a single part silver epoxy paste using a 152.4 µm syringe needle. After folding the substrate in a space saving state, a 60 °C heat source returns the shape memory polymer back to its printed permanently stored state. This demonstrates the possibilities of integrating shape memory polymers into packaging for the first time, while enabling future applications with heatsinks, origami meta-materials, and additional reactive and compact structures.**

Keywords-3D printing, 4D printing, Shape Memory Polymers, PLA, Antenna Array, Ka-band, Origami

I. INTRODUCTION

As additive manufacturing becomes increasingly used in industry practices, new techniques and designs will be explored that allow the creation of systems that were previously strenuous to manufacture. Engineers have been focusing on origami structures to allow designs that can be actuated while retaining high strength properties. For RF devices, origami-inspired designs present themselves as a solution to drastically reduce the footprint of RF devices and antennas while allowing for a real-time tunability and shape reconfigurability.

While 3D printing technology has been around since the 1980's, the once rapid-prototyping technique has rapidly gained attention with the expiration of patents and has become a manufacturing process for a variety of products. A variety of 3D printing techniques exist, from semiconductor scale metallic objects with minimum features of 30 µm and +/- 0.2 µm to Fused Deposition Modeling (FDM) 3D printing with 150 µm XY minimum features and 20 µm resolutions [1]. With conductive, flexible, and even materials that retain memory (4D printing), a limitless amount of designs can be manufactured. More importantly, these resolutions and a wide library of materials make this additive manufacturing technology viable for high frequency antenna design and packaging.

In this paper a method of low-cost 3D printing is investigated in the fabrication of high frequency antennas with configurability derived from thermoplastic shape memory polymers interacting with a commercial chip package.

II. MATERIAL CHARACTERIZATION

Currently, RF design is centered around the utilization of widely available, broadband characterized substrate in order to create designs with minimal variation between modeling and fabrication. The materials that make up these substrates are cheap in bulk, available from a wide range of sources, though typically purchased from a vender which focuses on consistent electromagnetic properties.

With the rapidly evolving field, there currently exist very few standards for 3D printable materials. Stereolithography printers (SLA) and multi-jet/polyjet 3D printers, for example, use multi-component proprietary formulas photopolymer resins that tend to exhibit higher losses than thermoplastics [2]. FDM printers often to use moderately simple thermoplastics that are generally single component, with a low percent weigh of optionally added colored die, often less than 5 %.

A. Ring Resonator Design

For designing any RF device on a new substrate, a characterization of some sort should be performed in order to verify assumed dielectric properties. A wide variety of methodologies exist for characterization. One method is the utilization of specific patterns that are metalized directly onto the substrate, such as T-resonators and ring-resonators, in order to view discrete points based on the order of resonance to extract the dielectric constant and loss tangent and interpolate between measured points. In order to verify the dielectric properties of the 3D printed PLA, a ring resonator design is employed.

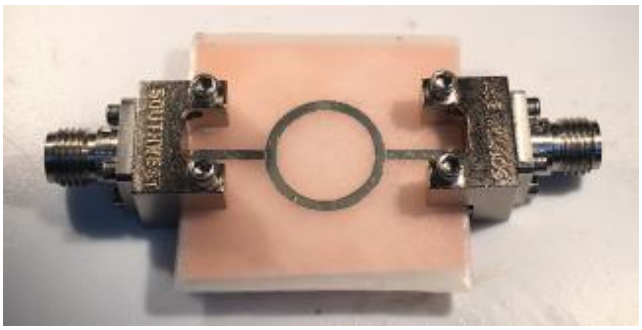

Figure 1. Ink-jet printed ring resonator with Southwest Microwave End Launch connectors.

2377-5726/17 $31.00 © 2017 IEEE
DOI 10.1109/ECTC.2017.186

In order for accurate extraction of loss tangent, surface roughness must be considered with respect to the skin depth of the conductor. With the measurement of the surface roughness demonstrated later, the roughness of FDM printable materials can often exceed the skin depth of conformal high conductivity materials at these frequencies and will influence the measured loss tangent.

A ring resonator is designed to have its first resonance at 4.84 GHz. To realize this resonant frequency, a 1 mm substrate with assumed dielectric constant of 2.7 has a line width of 1 mm for both the feeding microstrip line and ring, yielding an intrinsic impedance of 87.3 Ω which reduces dispersion versus a 50 Ω line [3]. The ring diameter from the center of the microstrip is 6 mm, with a 100 µm gap from edge of the ring to the feeding line. The design is printed on a 30 by 30 mm PLA substrate utilizing a Dimatix 2831 ink-jet printer with silver nanoparticle (SNP) ink. Four layers of SNP ink are printed with 20 µm drop spacing. As the SNP ink needs to be sintered at 120 °C to improve conductivity, the four corners are taped down to a glass carrier to prevent warping while the PLA heats up past the glass transition temperature (60-70 °C), but remains below the melting temperature (170-190 °C). The substrate is set into the oven while the oven is at room temperature to reduce thermal shock which tends to increase warpage. This method of metallization is only recommended for simple dielectric designs that have no overhang, and is therefore suitable for rapid prototyping of high resolution conductive inks on FDM printed rectangular parallelepiped substrates. The substrate with SNP is sintered for two hours at 120 °C and then allowed to cool down slowly at the same rate as Blue M oven.

B. *Ring Resonator Measurements*

The ring resonator is mounted with Southwest Microwave end launch connectors and measured from 2-30 GHz using an Anrtisu 37369A VNA. The measured S21 demonstrated three peaks at 10.90, 22.22m 29.67 GHz. Utilizing these peaks, an effective dielectric constant of 2.49, 1.15 and 1.15 is extracted at each respective frequency. Utilizing a width-height ratio of 1, the dielectric constants of the measured resonances are 3.33, 1.23, and 1.23.

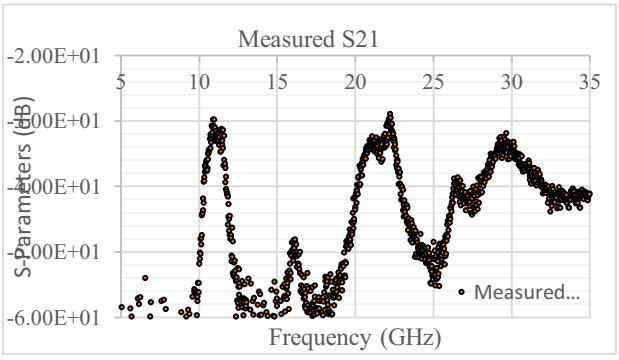

Figure 2. Measured S21 of ring resonator from 5-35 GHz.

III. ANTENNA DESIGN

A. *Single Antenna*

The trapezoidal planar monopole has an inherit wide bandwidth. The taper aides in a creating a compact wideband antenna that can be relatively forgiving with minor variances in manufacturing. In this design, the large end of the trapezoid is 2.47 mm, the small end .41 mm, and a length of 1.77 mm between these dimensions. The length of the transmission line is 9.90 mm, designed with a length to account for the end launch connector needed to verify the physically fabricated model. The 3D printed dielectric is polylactic acid (PLA) which will be discussed later. The simulated electrical properties are ε_r=2.7, tanδ=.007. These results were based off of correlation of loss tangent with frequency for thermoplastic polymers and a related characterization of PLA, before the ring resonator characterization [4], [5]. The physical model and related s-parameters can be seen in Figure 3 and 4.

Figure 3. Simulation of 3D printed trapezoidal monpole antenna.

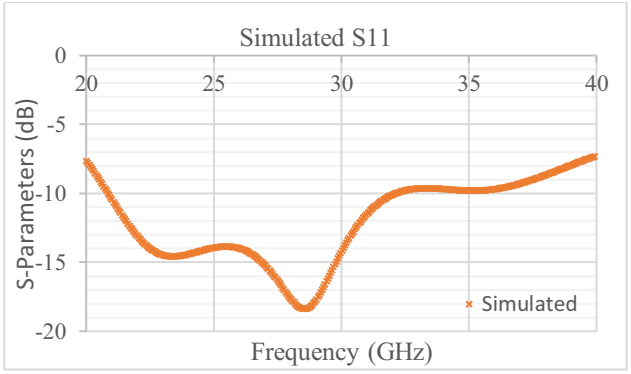

Figure 4. S11 of single antenna.

B. *Array Design*

A proposed antenna array is displayed, but the S parameters are not measured due to additional equipment or a redesign needed to make the 4 individual ports accessible for measurements. The design used to demonstrate the foldability and deployment of antennas, folding up similarly to the top of a packaging container. The designed dimension are 12mm x

12mm x .5 mm for the base's width, length, and height to match the Broadcom BCM2835 SoC as a heat source for deployability, as well as having adequate room for each individual antenna.

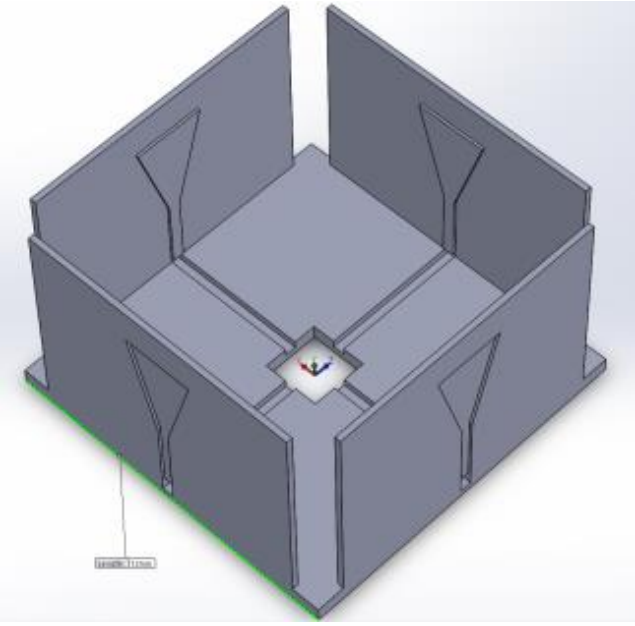

Figure 5. Quad monopole folding array.

IV. 3D PRINTING

There are a variety of 3D printing techniques. Historically, many were created for prototyping purposes to allow small scale manufacturing of new designs. All of them generally involve a technique called 'slicing,' which converts a 3D solid model into a computer-aided manufacturing (CAM) file that is composed of layers. The most common cited resolution is the height of each layer, often in the range of 20-300 microns depending on the manufacturing method, with the most advanced techniques reaching resolutions below .1 µm or lower. Different removable support materials or structures may be required depending on the process [6].

A. FDM Printing

Fused Deposition Modeling is the most common 3D printing technique, gaining popularity recently. The resolution of the layer height varies between 20-100 µm for most printers, often limited by the stepper motors and threading on the Z-axis. FDM printing functions by feeding filaments of thermoplastic polymers into a heated extruder that is on a XYZ moving platform. After the polymer exceeds the glass transition or melting temperature, the material is deposited. The minimum repeatable feature size is determined by the nozzle diameter. Many printers come with a diameter of .4-.5 mm, though in order to improve resolution and surface roughness, diameters of .2 mm can be obtained for consumer model printers. In order to see the viability of metalizing, measurements with this nozzle demonstrates a surface variation below 10 µm, as seen in Figure 6, which can exceed that of other higher resolution printing methods [7].

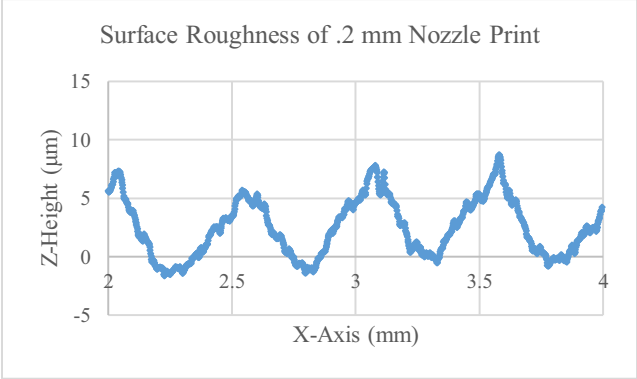

Figure 6. Surface Roughness Comparison

While the resolution and surface roughness may not be as precise as with other 3D printing techniques, the simplicity in the FDM process enables the capability to use multiple nozzles simultaneously, allowing multiple materials and different technologies such as Drop-On-Demand (DOD), Direct Printing Additive Manufacturing (DPAM), or laser sintering tools to coexist on a single platform allowing complex conductive, multimaterial structures. A large selection of filaments are available, such as ABS, PLA, HIPS, polyurethane, and composites are available consisting of PLA or ABS combined with copper, bronze, wood, iron, steel, carbon fiber, and ceramics. Custom materials can be fabricated with the appropriate tools and mixed during printing. While the material library is large, only a minority have been characterized up the RF frequency range [4, 5, 8].

B. Design Considerations

Creating a large scale visual replica with a 3D printer is relatively easy, but achieving ideal features for RF designs takes a significant amount of parameter adjusting. For this design, a low cost $399 Printrbot Play is used to demonstrate pushing consumer grade 3D printers to the limits to prototype RF designs. The Printrbot Play is outfitted with a non-standard .2 mm nozzle to increase the print resolution to a minimum feature size of .2 mm. Along with this metric, the minimum height the platform rises with a full step of the controller stepper motor (or linear actuator) which is an important factor for quality. This was determined to be .127 mm.

In order to achieve a Ka-band antenna that exceeds 26.5 GHz, considerations must be made for how the model will be converted from the 3D model to the machine code. While the nozzle diameter is the lower boundary of the width of a single extruded trace, the size may be increased up to approximately twice the size of the nozzle diameter. The width of the printed traces is called the extrusion width, and the design and the extrusion width should ideally be a multiple of each other, though many slicers automatically adjust the width to better fit and get the the most non-porous design. The height should also be a multiple of the determined lowest full-step.

In order to create the highest quality print in this design, the substrate is printed vertically. The conductor is inset 100 μm into the dielectric, and the substrate is designed to conform to the inset in order to make a uniform extrusion width print, as seen in Figure 7. The material is printed at 190 °C, at 30 mm/s to obtain an acceptable print quality. Increasing temperature increases layer-to-layer adhesion but eventually comes at a cost of lower print quality.

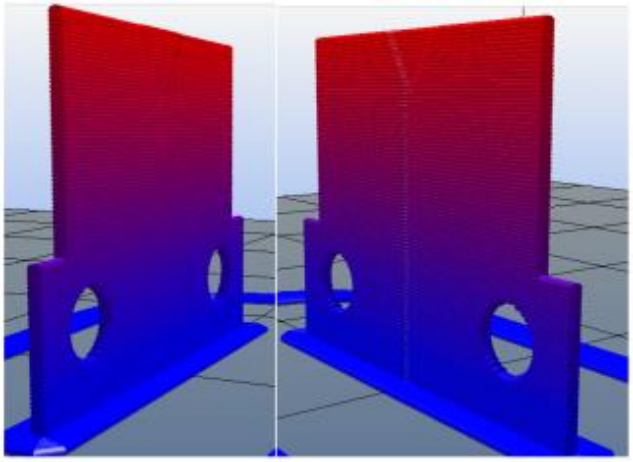

Figure 7. 3D model after being 'sliced' into layers

C. DPAM Metalization

In order to metalize the antenna onto the dielectric, direct print additive manufacturing is used (DPAM), a technique that involves using a dispensing tool on an XYZ platform. While specialized printers exist for this purpose, this design was metalized with a secondary 3D printer Hyrel System 30 with syringe dispensing capabilities. During the time of these measurements, the original printer's manufacturer has since released a syringe dispenser for their line of printers.

D. Materials

Polylactic acid (PLA) is used for its shape memory effects, while Atomic Adhesives AA-905 single part silver epoxy paste is used to create the antenna and microstrip line [9]. The polylactic acid properties of ε_r=2.7, tanδ=.007 were used [5].

The single part epoxy AA-905 has a variety of properties, discussed in fig 6. Notably, it is rated to be dispensed with a 30 AWG (.1524 mm) diameter. The curing temperature and times are modified to prevent any permanent deformation in the PLA, curing at temperatures below 120 °C. Diamine silver acetate with its ability to air cure without baking was attempted but was difficult to control spreading when dispensed through a syringe.

AA-905 Properties	
Sheet Resistivity	10-12 mΩ/sq
Viscosity @ 25 °C cps	6,800
Silver , %	70-72
Thermal Conductivity	4 W/(m*K)

Figure 8. List of AA-905 Properties [AA-905].

E. Shape Memory Effects

Certain polymers feature characteristic shape memory effects (SME), adequately called shape memory polymers (SMP). Specifically, shape memory materials are "smart" materials which recover from a temporary deformed shape to their original permanent shape. This allows printing in another dimension, time, that can be exploited with 3D printing to allow a controllable angle of actuation, providing microwave devices with an easy-to-control configurability up to an unprecedented degree, thus allowing for real-time frequency and direction tuning, extreme miniaturization and portability as well as real time control of radiation patterns and direction to dramatically improve energy harvesting and signal strength capabilities. While many SMP are thermo-responsive, technologies for shape memory include shape memory alloys (SMA) and photopolymers. With 3D printing, fully 3D hinging and origami shapes can easily be fabricated at room temperatures and the SMA designs are rigid for various intermediate shapes. After heating PLA near its glass transition temperature (65 °C) the material is pliable into a new temporary design which will be retained after heat is removed. If heat is introduced to the system again, the design will transition to its original permanent state. This can be seen in the physical model in Figure 8.

Figure 9. Shape Memory Polymer in permanent (top) state, temporariy (middle), and recovery to permanent (bottom) states after SoC acitvity.

V. RESULTS

The antenna was manufactured using the described methods. To expedite the manufacturing process, the large surface area ground plane was metalized using simple copper tape, and the simulation results were updated to reflect the change. Refer to figure 9, the results seem adequate with an approximate 7.5% shift in frequency likely due the unavailability of a wideband frequency characterization of the dielectric constant of PLA, which will be reserved for future research. The folded origami array was attached to a BCM2835 with double sided coppper tape, and began deploying when the chip heated to 62 °C.

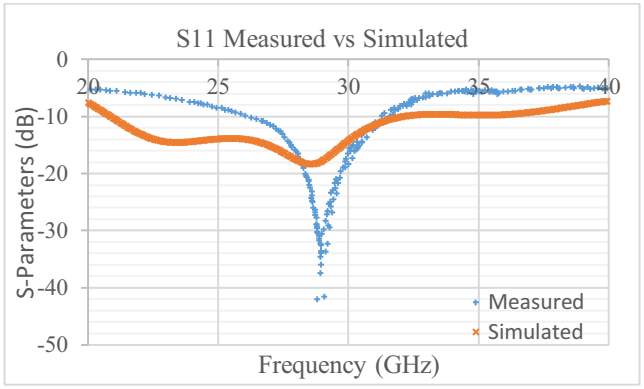

Figure 10. Measured S11, centered at 28.8 GHz with -40 dB

Figure 11. Single Antenna with Southwest Microwave Connector for S-parameter measurements.

VI. CONCLUSION

While this paper focuses on the abilities of a non-expensive consumer grade paper, further testing with higher end printers is necessary for design verification and would be beneficial. The ability to generate reactive 3D printed designs and metalize them with a single low-cost machine allows for the prototyping of unique new packages that can extend antenna arrays for energy harvesting, or possibly applications for reactive heatsinks or exposing a variety of sensors within the package according the environment [10].

With the rapid advancement of state-of-the-art 3D/4D printing technologies, new microwave devices are developed for applications that enable new dimensions: actuating, compact, wireless designs improving operability of the devices for systems and packages. With a wide range of freedom in design, a growing library of materials, and constantly improving resolution and accuracy, AM will remain a prime method in the manufacturing of novel microwave devices.

ACKNOWLEDGMENT

The authors would like to acknowledge the National Science Foundation (NSF) for their support with this work.

REFERENCES

[1] Cohen, Adam. “MICA Freeform vs Selective Laser Melting,” Online: http://www.microfabrica.com/downloads/MIC-WhitePaper-2014.pdf

[2] P. I. Deffenbaugh, R. C. Rumpf and K. H. Church, "Broadband Microwave Frequency Characterization of 3-D Printed Materials," in *IEEE Transactions on Components, Packaging and Manufacturing Technology*, vol. 3, no. 12, pp. 2147-2155, Dec. 2013.

[3] D. C. Thompson, O. Tantot, H. Jallageas, G. E. Ponchak, M. M. Tentzeris and J. Papapolymerou, "Characterization of liquid crystal polymer (LCP) material and transmission lines on LCP substrates from 30 to 110 GHz," in *IEEE Transactions on Microwave Theory and Techniques*, vol. 52, no. 4, pp. 1343-1352, April 2004.

[4] Deffenbaugh, Paul Isaac,”3D Printed Electromagnetic Transmission and Electronic Structures Fabricated on a Single Platform using Adavanced Process Integration Techniques”. Dept. of ECE, Univ. of Texas, El Paso, TX, 2014.

[5] S. Zhang, C. Njoku, W. Whittow and J. Vardaxoglou, "Novel additive manufactured synthetic dielectric substrates," *Radio Science Meeting (Joint with AP-S Symposium), 2015 USNC-URSI*, Vancouver, BC, Canada, 2015, pp. 21-21.

[6] Wood, Lamont. Baya, Vinod. “The role materials play in powering the 3-D printing revolution” http://www.pwc.com/us/en/technology-forecast/2014/3dprinting/ features/materials-3d-printing-revolution.html

[7] Nate, Kunal A.; Hester, Jimmy., et al. "A fully printed multilayer aperture-coupled patch antenna using hybrid 3D / inkjet additive manufacturing technique," in Microwave Conference (EuMC), 2015 European, vol., no., pp.610-613, 7-10 Sept. 2015

[8] Bahr, Ryan, et al. "RF characterization of 3D printed flexible materials - NinjaFlex Filaments," in Microwave Conference (EuMC), 2015 European, vol., no., pp.742-745, 7-10 Sept. 2015

[9] https://www.atomadhesives.com/AA-DUCT-905-Conductive-Micro-Application-Silver-Epoxy-Adhesive

[10] J. Kimionis, M. Isakov, B.S. Koh, A. Georgiadis, and M.M. Tentzeris, “3D-printed Origami Packaging with Inkjet-printed Antennas for RF Harvesting Sensors,” IEEE Transactions on Microwave Theory and Techniques (TMTT), vol.63, no.12, Dec. 2015